

## Article

# Experimental Investigation on the Effects of the Geometry of the Pilot Burner on Main Flame

Cheol Woo Lee <sup>1</sup>, In Su Kim <sup>2</sup> and Jung Goo Hong <sup>1,\*</sup> 

<sup>1</sup> School of Mechanical Engineering, Kyungpook National University, Daegu 41566, Korea; kaeru07@hyundai-steel.com

<sup>2</sup> Environmental & Energy Planning Team Hyundai Steel, Dangjin 31719, Korea; 12insu@hyundai-steel.com

\* Correspondence: jghong70@knu.ac.kr; Tel.: +82-53-950-6570

**Abstract:** Various kinds of pilot burners were experimentally investigated to examine the effects of their geometry and their location relative to the main burner of a real size combustor. In addition, a wide range of fuel equivalence ratios were investigated to analyze the feasibility of the novel pilot burner for the conventional burner application. From the results, it is shown that the novel pilot burner with multi air holes had a thin, straight, long and stable pilot flame, while the conventional pilot burner had a thick, lifted, short and unstable flame. It is also shown that the novel pilot burner with an upper air flow hole had a straight pilot flame which led to less thermal damage to the burner combustor. This study suggests that not only pilot burner flame shape but also the vertical location of the pilot burner from the main burner combustor has a significant effect on combustor durability.

**Keywords:** pilot burner; flame shape; burner geometry; flame temperature; buoyancy effect; thermal damage



**Citation:** Lee, C.W.; Kim, I.S.; Hong, J.G. Experimental Investigation on the Effects of the Geometry of the Pilot Burner on Main Flame. *Energies* **2021**, *14*, 1115. <https://doi.org/10.3390/en14041115>

Academic Editors: Wojciech Nowak, Jaroslaw Krzywanski and Karol Sztékler

Received: 6 January 2021

Accepted: 15 February 2021

Published: 20 February 2021

**Publisher's Note:** MDPI stays neutral with regard to jurisdictional claims in published maps and institutional affiliations.



**Copyright:** © 2021 by the authors. Licensee MDPI, Basel, Switzerland. This article is an open access article distributed under the terms and conditions of the Creative Commons Attribution (CC BY) license (<https://creativecommons.org/licenses/by/4.0/>).

## 1. Introduction

Pilot burner flame is one of the most important operating factors in many industrial furnaces since it influences not only product quality but also cost price. The geometry of pilot burners and their relative location from the main burner are much more important for the long-term operation of the continuous annealing line since both burners are encapsulated in a narrow radiant tube, which makes combustion phenomena and the gas dynamic more complicated. Elbaz et al. [1] performed an experimental research for partially premixed turbulent flames in order to investigate the effect of the coflow on the flame stability and flame structure. For example, a swirler has been a widely used representative tool to improve combustion stability and combustion efficiency simultaneously since it can stabilize flame with the help of recirculation zone and promote homogeneous air/fuel mixing. Pilot burners, therefore, need to be robust and flawless to avoid thermal damage or thermal deformation due to direct flame impingement onto the combustor. Many researchers have studied the effect of burner geometry on flame shape and its stabilization condition Aggarwal [2] conducted numerical and experimental research for extinction and blowout of laminar partially premixed flames that was motivated by considerations of fire safety and suppression. Syred [3] studied the swirl combustion system which allows coupling between the acoustics, combustion and swirling flow dynamics to occur. Lee et al. [4] investigated combustion instabilities, which were observed for various combustion geometries and operating conditions and which fundamentally consist of interactions between acoustic pressure waves and heat release. Masri et al. [5] studied experimental works on laboratory-scale swirl flame burners where significant reporting of results or data bases exists. This study focused on selected gaseous fuel burners that span premixed, partially premixed and non-premixed combustion over unconfined and confined conditions. Leung et al. [6] experimentally examined a premixed flame and an inverse diffusion flame in order to obtain information on their thermal, emission and

heat transfer characteristics for two swirl-stabilized flames. Galley et al. [7] investigated a laboratory-scale swirling burner, presenting many similarities. Lee et al. [8] studied the characteristics of partially premixed turbulent flames. They were investigated using a burner design that allows for a variation in the level of premixing between fuel and air. Some have reported that too strong a swirl intensity with a swirl number of more than 3 has shown unstable flame and carbon monoxide (CO) formation, which results from a flame quenching effect caused partly by strong momentum of combustion air and partly by incomplete combustion due to a significant amount of inert gas of burnt gas. Yang et al. [9] studied the influence of fuel preparation, combustor geometry, and operating conditions on combustion characteristics in a swirl-stabilized combustor.

Meanwhile, another important factor that influences flame stability is nozzle geometry. Mansour et al. [10] investigated flame stability and mean structure of partially premixed flames under the effect of partial premixing level and nozzle cone angle. Their experimental results showed that cone angle has a great influence on flame stability. Increasing the cone angle leads to more air entrainment, breaking the stabilization core and hence reducing flame stability. Akbarzadeh and Birouk [11] performed an experimental research to study the effect of fuel nozzle geometry on the stability of nonpremixed turbulent methane flame. They used four fuel nozzles, which were surrounded by an annulus of co-airflow, having a similar exit cross-sectional area but different internal/orifice geometries (circular, rectangular, square, and triangular). They concluded that the lift-off velocity did not change significantly with varying co-airflow rates. However, it was higher for the rectangular and triangular nozzles, followed by the square and circular nozzles. Paschereit et al. [12] reported that pilot flame affects low fields and combustion performances in a swirl-inducing burner. Their results suggest that at a constant total equivalence ratio, the injection of air through the pilot lance only showed better results than the pilot fuel and premixed pilot injection. Meares and Masri [13] introduced a modification of the well-known jet piloted burner to enable the stabilization of partially premixed flames with varying degrees of inhomogeneity in mixture fraction or equivalence ratio. From their results, it was found that flame stability was significantly improved due to inhomogeneity such that for intermediate recession distances in the range of 50–100 mm and for the same fuel equivalence ratio, the blow-off limits for the FJ cases (where fuel was injected into the inner pipe and air into the annulus) were more than 50% higher than those of the FA counterparts (where fuel was injected into the annulus and air into the inner pipe). Wang et al. [14] investigated the potential role that the diameter of a burner plays in flame structure and flame instability and the influence of burner diameter on the turbulent premixed flame structure.

Recently, Yu et al. [15] studied the effect of pilot flame on a piloted jet flame. They reported that the reaction zone of the piloted jet flame was in the mixing layer of the main jet and the hot coflow from the pilot flame. The equivalence ratio in the reaction zone could be significantly higher than that in the fuel/air mixture of the main flame, especially for the main flame that had a much higher equivalence ratio than that of the pilot flame. They also reported that the burning velocity of the main flame was insensitive to the hot gas composition from the pilot flame, indicating that the heat transfer from the pilot flame to the main flame had a more significant impact on the main flame than the transfer of radicals and combustion intermediates (such as CO and H<sub>2</sub>) from the pilot flame to the main flame.

Few researchers, however, have studied the effects of pilot burner nozzle geometry and equivalence ratio on pilot flame. In this study, therefore, the burner geometry and fuel equivalence ratio of the pilot burner were changed to investigate their effect on the pilot flame systematically. In addition, the distance between the pilot burner and the main burner was also varied to experimentally investigate its effect on main flame. Pilot burner geometry and fuel equivalence ratio affects pilot flame structure, thus making flame length longer and flame temperature higher for the worst case. It eventually leads to significant deformation of the combustor tube and radiant tube, as seen in Figure 1 of actual tubes in

the industrial field. No researchers, however, have studied the relation between pilot flame and combustor deformation in detail for real industrial radiant tubes.



Figure 1. Deformation of radiant tube and combustor.

## 2. Experimental Techniques and Facilities

### 2.1. Experimental Apparatus

Figure 2 shows the experimental apparatus used in this study. Fuel as LNG (Liquefied Natural Gas) is supplied from the gas bomb (which is pressurized at 120 bar and depressurized at 1 bar at the bomb exit) to the burners through gas pressure regulator (Parker, Columbus, OH, USA) with the final pressure of 250 mmH<sub>2</sub>O. Air for the main burner is supplied from an air blower of 400 mmH<sub>2</sub>O of which rated power is 1.75 kW. Air for the pilot burner and center air is supplied from an air compressor (Hanshin Machinery, 4 HP, Ansan, Korea) via a gas pressure regulator with 200 mmH<sub>2</sub>O. Fuel and air quantity were controlled through mass flow controllers (Dwyer Instruments, Michigan City, IN, USA).

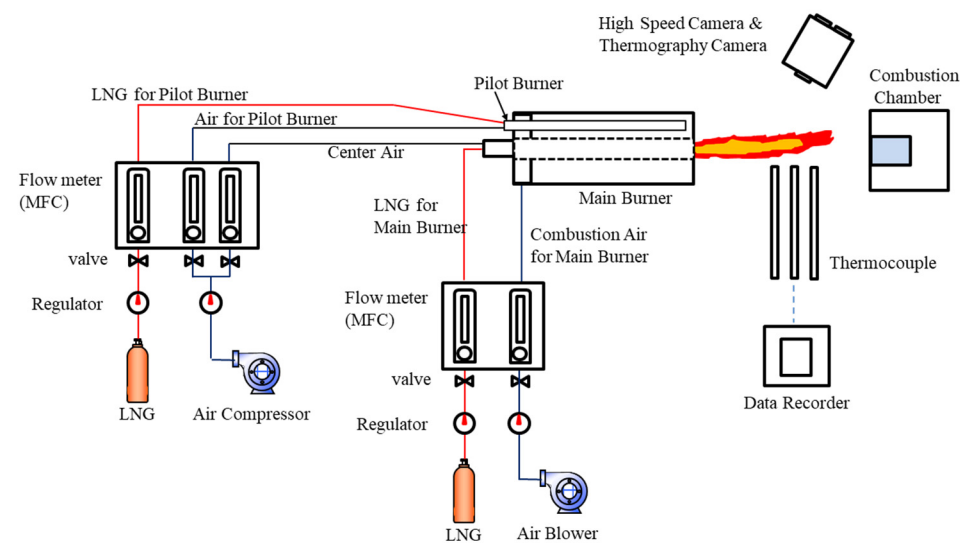


Figure 2. Schematic diagrams of experimental apparatus.

### 2.2. The Pilot Burner

Figure 3 shows various kinds of pilot burners used in this study. Four types of pilot burners were tested in this study. The type I pilot burner is an original pilot burner in which fuel and air are premixed. Type II is a new pilot burner for partially premixed flames which aims to reduce the buoyance effect by suppressing flame rise with upper holes of air addition. Type III is also a new pilot burner for partially premixed flames which aims to have the same effect as the Type II pilot burner but in which air is added from the bottom holes to prevent delayed pilot combustion. Finally, the Type IV pilot burner was designed to investigate the enhanced mixing effect of air addition from upper and bottom air holes.

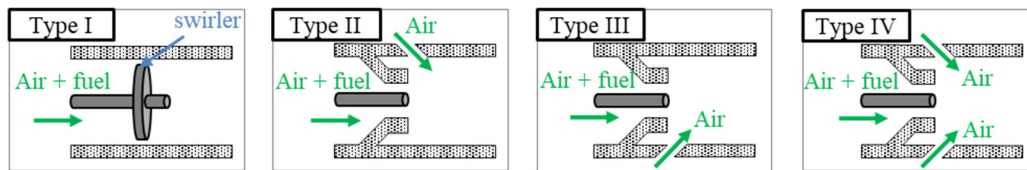


Figure 3. Schematic of used pilot burners.

### 2.3. The Main Burner

Figure 4 shows a radiant tube and an overall burner structure tested in this study. As described above, the pilot fuel and pilot air of the pilot burner flow through the pilot burner and those of the main burner flow through the main burner. As seen from Figure 2, the entire burner is encapsulated with a radiant tube. Flame photos and temperature were taken by using a high-speed camera and thermography camera (Photron, FASTCAM SA3, Tokyo, Japan). The low calorific value of LNG was  $42.6 \text{ MJ/Nm}^3$ , and its major composition is presented in Table 1.

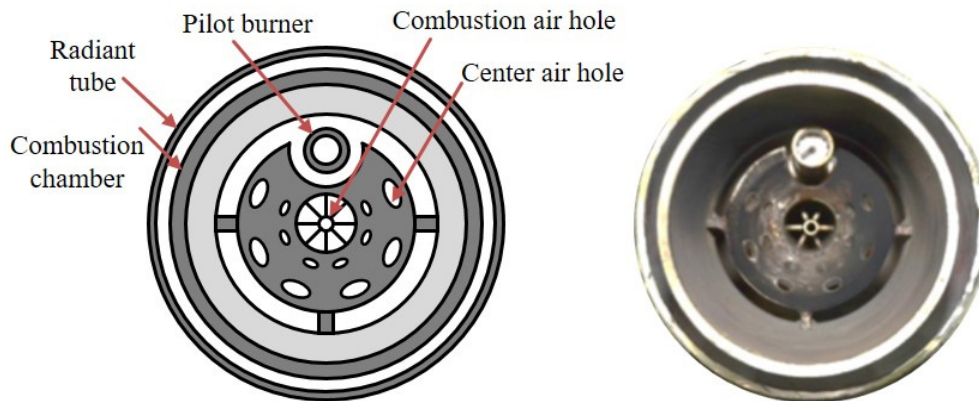


Figure 4. Schematic and a photo of used main burner (Bloomeng, 2320 Series, Pittsburgh, PA, USA).

Table 1. LNG (Liquefied Natural Gas) composition.

Element	Unit	
$\text{N}_2$ (Nitrogen)	% mol.	0.12
$\text{CO}_2$ (Carbon Dioxide)	% mol.	0.00
$\text{CH}_4$ (Methane)	% mol.	93.77
$\text{C}_2\text{H}_6$ (Ethane)	% mol.	3.80
$\text{C}_3\text{H}_8$ (Propane)	% mol.	1.67
$\text{I-C}_4\text{H}_{10}$ (Iso-Butane)	% mol.	0.29
$\text{N-C}_4\text{H}_{10}$ (Normal-Butane)	% mol.	0.32
$\text{I-C}_5\text{H}_{12}$ (Iso-Pentane)	% mol.	0.02
$\text{N-C}_5\text{H}_{12}$ (Normal-Pentane)	% mol.	0.00

### 2.4. Experimental Techniques

Fuel and air flow rates for the main burner were fixed to  $11$  and  $125 \text{ Nm}^3/\text{h}$ , respectively. Center air flow rates were set to  $4$ ,  $7$ , and  $10 \text{ Nm}^3/\text{h}$  with a total air flow rate of  $125 \text{ Nm}^3/\text{h}$  to investigate the effect of center air momentum on main flame shape. Moreover, to investigate the effect of air velocity on pilot flame shape, fuel flow rate for the pilot burner was fixed to  $0.2 \text{ Nm}^3/\text{h}$  and that of air was varied to correspond to a fuel

equivalence ratio of 0.8–2.5. K-type thermocouples were used to measure the temperature of the main flame and combustion chamber surface. A high-speed camera (Photron, FAST-CAM SA3, Japan) was used to take photos of some flames. The conditions used for the experiments are shown in Table 2.

**Table 2.** Experimental conditions.

Type	LNG Flow Rate (Nm <sup>3</sup> /h)	Combustion Air Flow Rate (Nm <sup>3</sup> /h)	Center Air Flow Rate (Nm <sup>3</sup> /h)
Main Burner	11	125	4
			7
			10
Pilot Burner	0.2	Fuel equivalence Ratio: 0.8–2.5 (Variables)	

### 3. Results and Discussion

Pilot burner position was considered to be one of the most important factors affecting combustion chamber durability since the pilot flame together with the main flame impinged the inner wall of the combustion chamber, which resulted in deformation of the combustion chamber as shown in Figure 5. Thus, the distance between the center of the pilot burner axis and the main burner was varied from 30 to 50 mm. Figure 6 shows images of infrared thermography at the combustion chamber taken by an infrared thermography camera (FLIR, T365, Wilsonville, OR, USA).



**Figure 5.** An example of the combustion chamber deformation by flame.

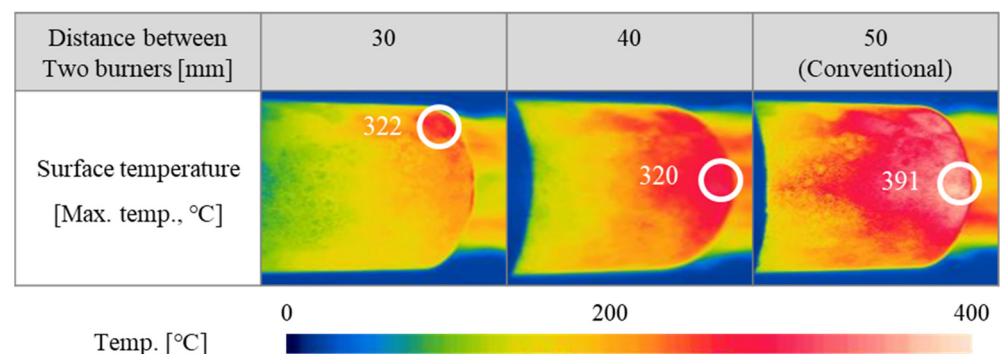


**Figure 6.** Results of infrared thermography at the combustion chamber.

The maximum surface temperature of the combustion chamber was reached when the distance between two burners was 50 mm. This phenomenon is considered to be mainly due to the proximity of the pilot burner to the combustion chamber. Hence, pilot flame directly impinges on the combustion chamber due to the buoyancy effect, which leads to higher surface temperature of the combustion chamber. Meanwhile, surface temperature of the combustion chamber was lowest when the distance between two burners was only

30 mm. This means that when the pilot burner has enough distance from the combustion chamber, it is likely that the pilot flame does not impinge on the combustion chamber.

The maximum temperature for this case, however, was over 300 °C, which can still cause burner deformation due to local impingement of pilot flame on the combustion chamber. Thus, the fundamental solution for preventing pilot flame impingement on the combustion chamber was to avoid the flame buoyancy effect [16] through adequate pilot burner geometry. Rokke et al. [17] investigated unconfined turbulent partially premixed propane/air flames issuing from a straight tube into quiescent air at atmospheric pressure and temperature. Experiments on lifted flames are performed.

Figure 7 shows photos of flames for type I and type IV pilot burners when the fuel equivalence ratio was changed from 0.8 to 2.5. The flame length ( $\ell$ ) of the type I pilot burner was obviously shorter than that of the type IV pilot burner over the fuel equivalence ratio range used. This resulted from the existence of a swirler in the type I pilot burner since swirl flow rigorously promotes the mixing of air and flame and generates a recirculation zone which consequently leads to a shorter flame. Flame width, however, is thicker with the flame of the type I pilot burner over the fuel equivalence ratio range used due to swirl flow. In fact, flame widths were even twice or three times thicker with the type I pilot burner, which may cause pilot flame impingement on the combustion chamber. Considering that the possibility of flame impingement on the combustion chamber is higher with a thicker flame, the type IV pilot burner is preferable in terms of burner lifetime. Moreover, since the fuel and air of the main burner flow near the burner center, a long and slim flame is more likely to stabilize the main flame over the fuel equivalence ratio range used.

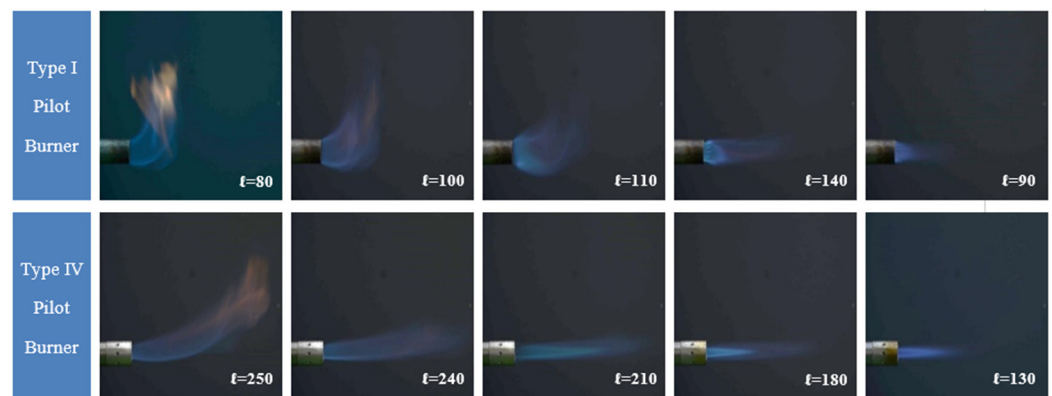


**Figure 7.** Comparison of flame shapes and length ( $\ell$ ).

Note that the fuel equivalence ratio range of 0.8–2.5 is mostly used in reality, that is, in the industry field. Flame lifting due to the buoyancy effect was considerably improved with the type IV pilot burner, but slightly lifted flame was still observed, which could cause combustion chamber deformation. Thus, the direction of the pilot air flow was investigated for a fuel equivalence ratio of 1.25 in terms of flame straightness, and the results are shown in Figure 8.

Flame shapes seem to be almost the same for all three air injection cases, except that upper injection has little effect on flame buoyancy. This is because upper injection prohibits the fuel–air mixture from burning on the upper region of the flame due to entrained air [18], i.e., it forcedly shifts the rich fuel–air mixture to the lower vertical part of the pilot burner through its momentum and dilution. As a result, in this study, no flame was observed within 5 mm of the upper nozzle region, as shown in Figure 8. Lower injection also showed no flame near the lower nozzle region. From these results, it can be inferred that upper injection is more effective in preventing combustion chamber deformation due to the pilot flame buoyancy effect.

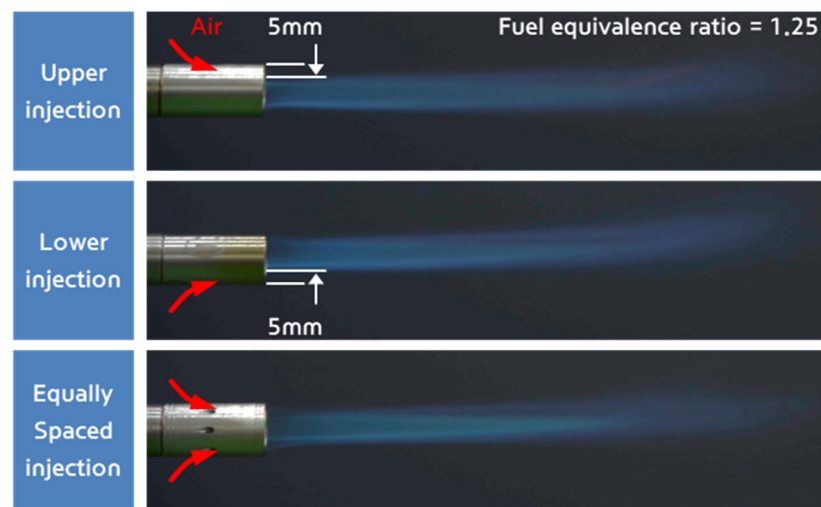


**Figure 8.** Comparison of flame shapes by air injection direction.

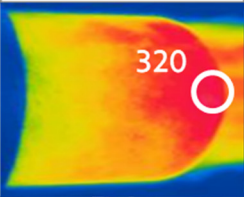
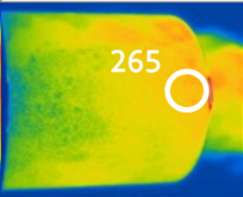
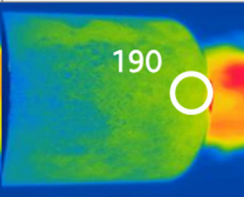
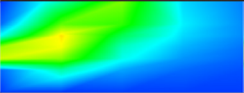
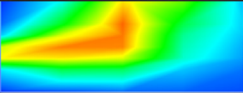
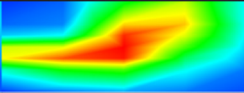
In the original pilot burner, pilot fuel and pilot air are relatively well premixed in the pilot burner; thus, most of pilot fuel and air are burnt before the pilot burner exit. This enhances chemical reactions of main fuel and air mixture. Thus, burnt gas quantity increases at the burner upstream, which means higher exhaust gas temperature. This leads to a buoyancy effect at the burner upstream for the original burner.

Meanwhile, pilot fuel and air for the novel pilot burner of type IV are burnt after pilot burner exit. Consequently, an earlier combustion reaction of the mixture of the main fuel and air is delayed, which may suppress the buoyancy effect of the flame.

Though pilot flame was improved through modification of the pilot burner geometry, the main flame is still another important factor that influences combustion chamber deformation. From this standpoint, center air flow rate was changed for the same test condition as that in Figure 6. Figure 9 shows the surface temperature, flame shapes, and flame temperature contours when the center air flow rates were 4, 7, and 10 Nm<sup>3</sup>/h.

From Figure 9, it is shown that the higher the center air flow rate, the smaller is the maximum surface temperature of the combustion chamber. In particular, the maximum surface temperature of the combustion chamber dropped drastically when the center air flow rate was 10 Nm<sup>3</sup>/h. Flame width, however, was narrower and the flame's hot region was wider, as represented by the red color on the flame temperature contour. This means that there is a possibility of higher NO<sub>x</sub> formation due to hot temperature. Meanwhile, a narrower flame is not preferable since heat transfer through heat radiation is more important than heat transfer through heat conduction and heat convection. Note that the burner investigated in this study was encapsulated in radiant tubes.

Finally, the novel pilot burner with increased center air flow rate and optimal pilot burner position of 40 mm was tested under atmospheric conditions to investigate its applicability in a real furnace system. From Figure 10, it is obviously shown that the maximum surface temperature of the combustion chamber drastically decreased due to improved flame structure. Through this sufficient laboratory experiment, it was applied to the actual site. This means that there will be no combustion chamber deformation due to flame impingement during the lifetime of the burner system.

Center air [Nm <sup>3</sup> / h]	4	7	10
Surface temperature Max. temp. [°C]			
Flame shape			
Flame temperature contour			
Max. flame temp. [°C]	778	899	998

**Figure 9.** Effect of center air volume on flame shape and its temperature. (Fuel equivalence ratio  $\phi = 1.25$ ).

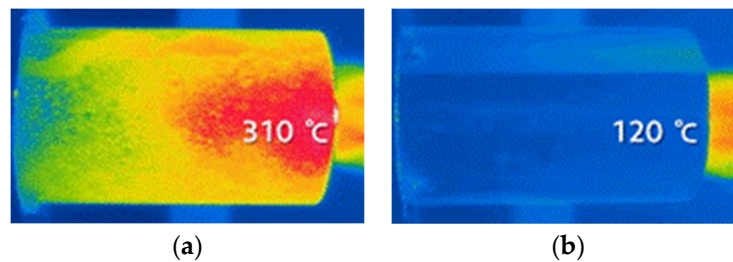


**Figure 10.** Comparison of surface temperature between (a) Conventional burner; (b) Novel burner.

Figure 11a shows flame image and flame temperature contours for an original burner, and Figure 11b shows those for the novel burner with the Type I pilot burner. As seen from flame image in Figure 11a, the bright area of the flame upstream is narrower than that of the flame image in Figure 11b. This may result from the fact that since pilot fuel and pilot air are well premixed in the pilot burner, the fuel air mixture is burnt more quickly in the original burner than the new novel burner. Thus, the flame is more lifted at the flame end for the flame image of the original burner in Figure 11a.

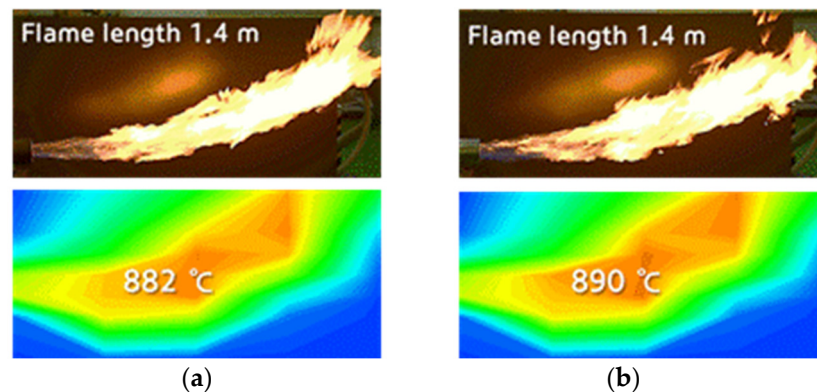


**Figure 11.** Comparison of flame shape and temperature between (a) Conventional burner; (b) Novel burner. (Fuel equivalence ratio  $\phi = 1.25$ )

Flame thickness in the middle position of the longitudinal flame image of the new novel burner in Figure 11b explains the above fact well. That is, wider flame thickness comes from relatively delayed combustion for the new novel burner from Figure 11b due to less premixed (partially premixed) combustion.

In addition, the flame temperature contours of new novel partially premixed pilot burner suggest that the flame thickness is wider and overall flame temperature is a little higher than those of the original premixed pilot burner, which coincides with previously described phenomena.

#### 4. Conclusions

The effects of the geometry and location of the pilot burner and the center air flow rate of the main burner on combustion chamber deformation due to flame impingement were experimentally investigated in this study. Images of the pilot flame and those of the main flame were taken, and the temperature of the combustion chamber and that of main flame were measured. Through this study, the following results were obtained:

- (1) There exists a certain distance (in this study, it is 40 mm) between the pilot burner and the main burner which can reduce main flame impingement onto the combustion chamber.
- (2) Upper injection of the pilot air prevents the flame buoyancy effect, which leads to longer use of combustion chamber without any combustion performance loss.
- (3) Center air flow rate of the main burner can also improve the flame buoyancy effect, which prevents flame impingement onto the combustion chamber.
- (4) The combination of the novel pilot burner and center air flow rate of the main burner can significantly reduce flame impingement. Thus, this novel burner system can be applied to a real furnace system.

**Author Contributions:** Conceptualization, methodology, validation, data curation, C.W.L. and I.S.K.; writing—original draft preparation, C.W.L.; writing—review and editing, I.S.K. and J.G.H.; supervision, J.G.H. All authors have read and agreed to the published version of the manuscript.

**Funding:** This research received no external funding.

**Institutional Review Board Statement:** Not applicable.

**Informed Consent Statement:** Not applicable.

**Data Availability Statement:** Not applicable.

**Conflicts of Interest:** The authors declare no conflict of interest.

#### References

1. Mansour, M.S.; Elbaz, A.M.; Samy, M. The Stabilization Mechanism of Highly Stabilized Partially Premixed Flames in a Concentric Flow Conical Nozzle Burner. *Exp. Therm. Fluid Sci.* **2012**, *43*, 55–62. [[CrossRef](#)]
2. Aggarwal, S.K. Extinction of Laminar Partially Premixed Flames. *Prog. Energy Combust. Sci.* **2009**, *35*, 528–570. [[CrossRef](#)]
3. Syred, N. A Review of Oscillation Mechanisms and the Role of the Precessing Vortex Core (PVC) in Swirl Combustion Systems. *Prog. Energy Combust. Sci.* **2006**, *32*, 93–161. [[CrossRef](#)]
4. Lee, S.Y.; Seo, S.; Broda, J.C.; Pal, S.; Santoro, R.J. An Experimental Estimation of Mean Reaction Rate and Flame Structure During Combustion Instability in a Lean Premixed Gas Turbine Combustor. *Proc. Combust. Inst.* **2000**, *28*, 775–782. [[CrossRef](#)]
5. Al-abdeli, Y.M.; Masri, A.R. Review of Laboratory Swirl Burners and Experiments for Model Validation. *Exp. Therm. Fluid Sci.* **2015**, *69*, 178–196. [[CrossRef](#)]
6. Zhen, H.S.; Leung, C.W.; Cheung, C.S. A Comparison of the Thermal, Emission and Heat Transfer Characteristics of Swirl-Stabilized Premixed and Inverse Diffusion Flames. *Energy Convers. Manag.* **2011**, *52*, 1263–1271. [[CrossRef](#)]
7. Galley, D.; Ducruix, S.; Lacas, F.; Veynante, D. Mixing and Stabilization Study of a Partially Premixed Swirling Flame Using Laser Induced Fluorescence. *Combust. Flame* **2011**, *158*, 155–171. [[CrossRef](#)]
8. Lee, T.W.; Fenton, M.; Shankland, R. Effects of Variable Partial Premixing on Turbulent Jet Flame Structure. *Combust. Flame* **1997**, *109*, 1175–1185. [[CrossRef](#)]
9. Huang, Y.; Yang, V. Dynamics and Stability of Lean-Premixed Swirl-Stabilized Combustion. *Prog. Energy Combust. Sci.* **2009**, *35*, 293–364. [[CrossRef](#)]

10. El-Mahallawy, F.; Abdelhafez, A.; Mansour, M.S. Mixing and Nozzle Geometry Effects on Flame Structure and Stability. *Combust. Sci. Technol.* **2007**, *179*, 249–263. [[CrossRef](#)]
11. Akbarzadeh, M.; Birouk, M. Liftoff of a Co-Flowing Non-Premixed Turbulent Methane Flame: Effect of the Fuel Nozzle Orifice Geometry. *Flow Turbul. Combust.* **2014**, *92*, 903–929. [[CrossRef](#)]
12. Emara, A.; Lacarelle, A.; Paschereit, C.O. Pilot Flame Impact on Flow Fields and Combustion Performances in a Swirl inducing Burner. In Proceedings of the 45th AIAA/ASME/SAE/ASEE Joint Propulsion Conference & Exhibit, Denver, CO, USA, 2–5 August 2009; p. 5015.
13. Meares, S.; Masri, A.R. A Modified Piloted Burner for Stabilizing Turbulent Flames of Inhomogeneous Mixtures. *Combust. Flame* **2014**, *161*, 484–495. [[CrossRef](#)]
14. Wang, X.; Cheng, X.; Lu, H.; Pan, F.; Qin, L.; Wang, Z. Effect of Burner Diameter on Structure and Instability of Turbulent Premixed Flames. *Fuel* **2020**, *271*, 536–548. [[CrossRef](#)]
15. Yu, S.; Bai, X.S.; Zhou, B.; Wang, Z.; Li, Z.S.; Aldén, M. Numerical Studies of the Pilot Flame Effect on a Piloted Jet Flame. *Combust. Sci. Technol.* **2019**. [[CrossRef](#)]
16. Tao, C.; Qian, Y.; Tang, F.; Wang, Q. Experimental Investigations on Temperature Profile and Air Entrainment of Buoyancy-Controlled Jet Flame from Inclined Nozzle Bounded the Wall. *Appl. Therm. Eng.* **2017**, *111*, 510–515. [[CrossRef](#)]
17. Rokke, N.A.; Hustad, J.E.; Sonju, O.K. A Study of Partially Unconfined Propane Flames. *Combust. Flame* **1994**, *97*, 88–106. [[CrossRef](#)]
18. Longhu, H.; Xiaochun, Z.; Xiaolei, Z. Flame Heights and Fraction of Stoichiometric Air Entrained for Rectangular Turbulent Jet Fires in a Sub-Atmospheric Pressure. *Proc. Combust. Inst.* **2017**, *36*, 2995–3002.